Available online at www.sciencedirect.com

SciVerse ScienceDirect

Procedia Engineering 42 (2012) 1840 – 1848

Procedia Engineering

www.elsevier.com/locate/procedia

20th International Congress of Chemical and Process Engineering CHISA 2012
25 – 29 August 2012, Prague, Czech Republic

The effects of surfactants on the drag of a bubble

J. Ramírez-Muñoz[a], O. G. Galicia-Nequiz[a], S. Baz-Rodríguez[b], J. A. Colín-Luna[a], S.A. Martínez-Delgadillo[c], H. Puebla[a] a*

[a]*Universidad Autonoma Metropolitana Azcapotzalco, Departamento de Energia, Av. San Pablo 180, Col. Reynosa-Tamaulipas, México D.F., 02200, Mexico*
[b]*Universidad Autonoma Metropolitana Iztapalapa, Departamento de IPH, San Rafael Atlixco #186, Col. Vicentina, México, D.F., 09340, Mexico*
[c]*Universidad Autonoma Metropolitana Azcapotzalco, Departamento de Ciencias Básicas, Av. San Pablo 180, Col. Reynosa-Tamaulipas, México D.F., 02200, Mexico*

Abstract

It is well-know that the presence of surfactant critically decreases the velocity of bubbles. This is explained by the Marangoni effect, which implies that the shear-free boundary condition imposed in the gas-liquid interface is no longer valid, and this leads to an increase in the drag force on the bubble. Most mathematical models proposed in the past to simulate the increase in the drag as a function of surface contamination assumes the stagnant cap hypothesis. In this work, the steady drag for spherical bubbles moving to its terminal velocity in a liquid contaminated with surfactants was obtained via numerical simulations for $50 \leqslant Re \leqslant 200$ by using Comsol Multiphysics® 3.5a with the stagnant cap hypothesis. Different levels of surface contamination from clean bubble up to fully contaminated bubble were considered. The numerical values of drag force, flow velocity and pressure fields as function of the grade of contamination and Re were examined. Additionally, the flow regime (*Re*) under which a recirculating zone is formed behind a spherical bubble is numerically determined for each extent of the angle of contamination. The agreement of the numerical results with reported drag values was proved. By using an appropriate normalization of the numerical data, a simple explicit drag law for contaminated bubbles as function of the stagnant cap angle was obtained.

Keywords: Bubble drag; Marangoni effect; contaminated bubbles; surfactant effect on bubbles

* Corresponding author. Tel.: +52 55-5318-9000; fax: +52 55-5394-7378.
E-mail address: hpuebla@correo.azc.uam.mx.

doi:10.1016/j.proeng.2012.07.579

1. Introduction

Bubble columns are widely used for conducting gas-liquid reactions in a variety of practical applications in industry such as absorption, fermentations, bio-reactions, coal liquefaction and wastewater treatment. In spite of its apparent simplicity, their analysis is still a difficult task and subject to errors, due to the generally complex structure of the multiphase flow encountered in this type of equipment and important aspects of the dynamic of bubbles remain uncertain. For instance, available measuring techniques of the drag force are well suited for the case of fixed spheres, but this is not the case for clean or contaminated rising bubbles. In particular, the determination of the drag force on a bubble rising in a liquid contaminated with surfactants is important for understanding the basic bubble behavior in relevant industrial applications.

For the dynamic description of gas-liquid flows, information regarding the drag forces between phases is required. Therefore, one of the main objectives of researchers in this field has been to obtain numerical values of the drag acting on bubbles rising in clean or contaminated liquids [1-3]. However, it is well-know that the presence of surfactant critically decreases the rising velocity of bubbles in contaminated water compared with bubbles rising in pure water [4-5]. Thus, while a spherical bubble rising in a contaminated liquid flow behaves liked a rigid sphere, a clean spherical bubble of the same size in an uncontaminated liquid behaves very different. The reason for this retardation is that adsorbed surfactant is swept by the advection to the trailing surface of the bubble where it accumulates and yield an uneven surface tension. This is lower in the back surface relative to the front end. The difference in tension creates a Marangoni force which opposes the surface flow, i.e. a tangential shear stress appears on the bubble surface, which increases the drag coefficient and reduces de rising velocity of the bubble [6]. At some point, a limit value of the rise velocity is reached, no longer affected by a further increase in concentration. In this limit, the rate of either kinetic or diffusive transport of surfactant to the bubble surface is slow relative to surface convection and surface diffusion is also slow, surfactant collects in a stagnant cap at the back end of the bubble while the front end is stress free and mobile [7]. Considering the mechanism that governs the phenomenon, in the literature, most mathematical models proposed to simulate the increase in drag coefficient as a function of surface contamination assumes the stagnant cap hypothesis [6-8], which was first proposed by Frumkin and Levich [9]. The stagnant cap regime has been successful in explaining experimental observations of bubbles rising in liquids contaminated with surfactants [7]. For instance, by successive adjustments of the contaminated angle the computations are able to reproduce properly experimental rise velocities of bubbles.

In this work, the steady drag for spherical bubbles rising in a liquid contaminated with surfactants was obtained numerically for $50 \leqslant Re \leqslant 200$ assuming the stagnant cap hypothesis and by using Comsol Multiphysics® 3.5a (Re is the Reynolds number defined through the bubble's diameter and single bubble rise velocity). By using an appropriate normalization of the numerical data, a simple explicit drag law for contaminated bubbles was obtained. In addition, the structure of the flow around the bubble as function of as function of Reynolds number and grade of contamination when is examined.

This work is organized as follows: In Section 2 problem formulation and numerical solution are presented. In Section 3 numerical results supported with previously reported numerical data and a drag law are presented. Finally in Section 4 some concluding remarks are provided.

2. A bubble rising in a contaminated liquid

In this section the problem formulation for a contaminated bubble moving to its terminal velocity is introduced and the governing equations for the case study are presented. The numerical solution is

described. Comparisons of the numerical results with expressions of the literature for clean bubbles and rigid spheres are also presented.

2.1. Problem formulation.

Consider a spherical bubble of diameter d, at rest in an infinite body of Newtonian moving fluid, as shown in Fig. 1. The uniform velocity far away from the bubble is u, and the flow is assumed to be axisymmetric. In order to simplify the analysis of the problem is assumed that the amount of surfactant collects in the stagnant cap at the back end of the bubble remain constant. Thus, θ is the angle between the front stagnation point and the current point on the interface, i.e. the region free of surfactants where a shear-free condition is imposed ($\tau_{r\theta}$=0), meanwhile θ_C =180-θ is the fully contaminated region with tangential velocity equal to zero (u_T=0).

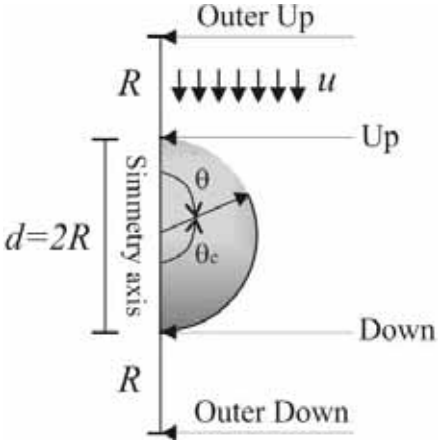

Fig. 1. Sketch of the problem and positions where velocity and pressured fields are evaluated.

Since it is assumed that the net mass transfer between the bulk and the bubble surface is neglected, the governing equations can be described by the full incompressible Navier-Stokes and continuity equations, written by

$$\frac{\partial \mathbf{V}}{\partial t} + \mathbf{V}\square\nabla\mathbf{V} = -\frac{1}{\rho}\nabla P + \nu\nabla^2\mathbf{V}\,, \tag{1}$$

$$\nabla\cdot\mathbf{V} = 0\,, \tag{2}$$

where $\mathbf{V}$, ρ and ν denotes the velocity field, the density and the kinematic viscosity of the liquid, respectively. Assuming that the bubble does not deform and that no phase change occurs, the normal velocity vanishes at the interface, i.e. $\mathbf{V}_n = u_n = 0$.

2.2. Solution of the model.

Numerical simulations were conducted for the axisymmetric flow around a spherical bubble for Reynolds numbers ranging between 50 and 200. The continuity and momentum equations (Eqs. 1 and 2) were solved under the assumptions of the stagnant cap model described above using the Comsol Multiphysics® 3.5a simulation code. A 2D geometry with axial symmetry was used and several types of

meshing were included in order to obtain independent results from the numerical parameters. Furthermore, an adaptive mesh refinement scheme was useful to ensure grid independence. Different levels of surface contamination, from clean bubbles (stagnant cap angle, $\theta_C=0^o$) up to fully contaminated bubbles (rigid spheres, $\theta_C=180^o$) were considered. Two boundary conditions in the gas-liquid interface were imposed in the simulations: 1) a region free of surfactants of angle θ, where a free-shear stress was imposed, and 2) a fully contaminated region of angle $\theta_C=180-\theta$ where a tangential velocity equal to zero was imposed.

The vertical component of the drag force on the bubble surface F_d was directly obtained from Comsol Multiphysics® 3.5a. The drag coefficient was calculated from its definition, given by [10]

$$C_{d,B}=\frac{F_d/\pi/4d^2}{1/2\,\rho U_b^{\,2}}\,. \tag{3}$$

2.3. Results validation.

Fig. 2 shows the variation of the numerical drag coefficient Cd as function of the bubble Reynolds number, Re, together with that for a clean bubble and a rigid sphere predicted by Moore and Clift given by

$$C_{d,B}=\frac{48}{\mathrm{Re}}\left(1-\frac{2.211}{\mathrm{Re}^{0.5}}\right) \tag{4}$$

and

$$C_{d,S}=\frac{16}{\mathrm{Re}}\left(1+0.1935\,\mathrm{Re}^{0.6305}\right), \tag{5}$$

respectively. As can be observed, the numerical data obtained with the Comsol Multiphysics® 3.5a simulation code are in very good agreement with both expressions.

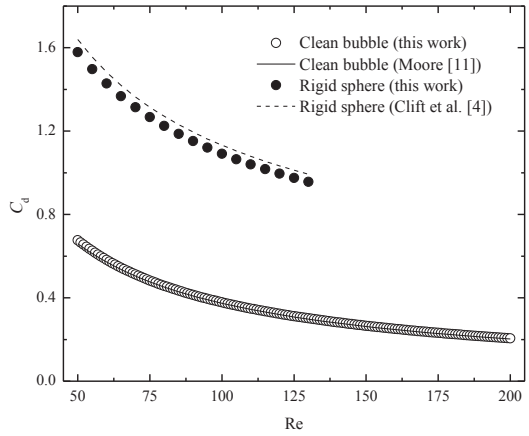

Fig. 2. Comparison of the numerical drag coefficients C_d obtained in this work for a clean bubbles and rigid spheres with that reported in the literature

3. Discussion and results

In this section obtained results for the drag, wake structure and velocity and pressure fields around the bubble are discussed.

3.1. Drag on a contaminated bubble.

Fig. 3 show the drag coefficient numerical values as function of the contaminated grade θ_C for $0 \leq \theta_C \leq 180$ and $50 \leq Re \leq 200$, which were normalized using the following expression [6]:

$$\frac{C_{d,CB} - C_{d,B}}{C_{d,S} - C_{d,B}}, \tag{6}$$

where $C_{d,CB}$, $C_{d,B}$ y $C_{d,S}$ are the drag coefficients for a contaminated bubble, a clean bubble and a rigid sphere, respectively. Fig. 3 also shows the numerical adjustment with numerical data obtained from Ec. (3), given by the following expression:

$$f(\theta) = \frac{1}{1 + \exp(-4.055\ \theta + 5.5466)}\ . \tag{7}$$

As can be seen, both qualitative and quantitative results are very promising with a 0.2 % average relative error. From Fig. (3) it can be observed that the drag coefficient values as a function of the angle of contamination θ_C shows a slight variations with *Re*. These results show that the drag of a contaminated bubble is nearly that of a clean bubble when $\theta_C < 30^o$ and that of a rigid sphere when $\theta_C < 135^o$. Between these bounds the drag is a strongly decreasing function of θ_C, with the maximum dependency being observed in the range θ_C=60-100°. These results are in agreement with the Sadhal & Johnson results in the creeping flow limit [12] and with the Cuenot et al. [6] results for Re=100.

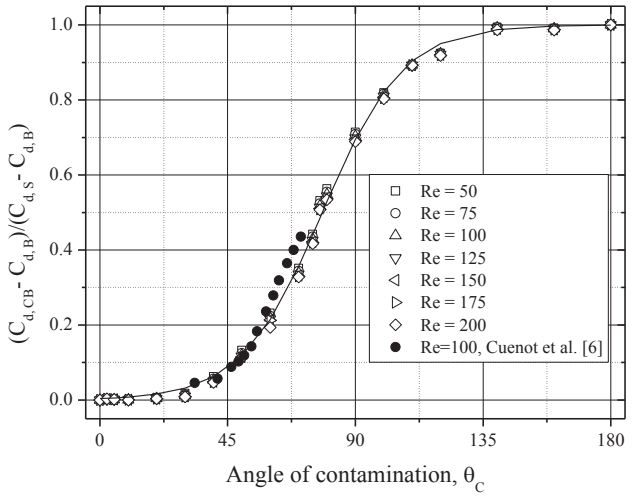

Fig. 3. Dimensionless drag coefficient as function of the contamination angle θ_C

3.2. Wake structure behind a contaminated bubble.

Fig. 4 shows the angle of contamination θ_C, at which is formed a recirculation region of length *R/10* as a function of *Re*, where *R* is the bubble radio. Results from Fig. 4 are useful to analyze the recirculation region in a systematic form. The distance *R*/10 can be considered as a characteristic length where the recirculation region is formed. Thus, seems to be suitable to introduce this distance as a reference to analyze the effect of surfactants on the bubble surface on the flow structure around the bubble. According to results show in Fig. 4 three regions can be identified: (i) a linear region, where is found a strong dependence of the *Re* with the angle of contamination ($\theta_C \leq 45^o$), (ii) a transition region, where this dependence gradually decreases ($45^o < \theta_C \leq 80^o$), and (iii) an asymptotic region, where the flow structure is independent of the contamination angle θ_C. It is noted that the numerical solutions derived considering the surfactant sorption kinetics between the bulk and the surface for $70° \leq \theta_C \leq 80°$, reaches a critical concentration of surfactants on the bubble surface, i.e. the bubble rise velocity remain constant and for greater stagnant angle values, approaches that of a rigid sphere [13].

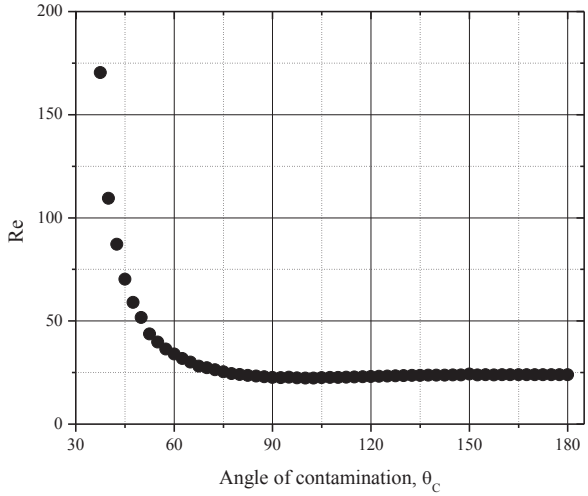

Fig. 4. Re value for each specific angle of contamination at which is formed a circulation region of length R/10

3.3. Velocity and pressure fields around the bubble

Figs. 5 and 6 show the pressure and velocity field distribution around the bubble for Re=100. Both images are illustrative of the contamination angle effect on the flow field at the two limit region showed in Fig. 3: $\theta_C=0^o$ and $\theta_C=45^o$ (Fig. 5a,b) and $\theta_C=135^o$ and $\theta_C=180^o$ (Fig. 6a,b). Fig. 5 shows that both the pressure and the velocity spatial distribution are very similar above the non-slip region for $\theta_C=0^o$ and $\theta_C=45^o$. However, the width of the wake (i.e. the total momentum loss of the fluid) behind the bubble is slightly greater for $\theta_C=45^o$ than $\theta_C=0^o$. Considering that the momentum deficit in the wake is equal to the drag force on the body [14, 15], this explains why the drag is greater for $\theta_C=45^o$. On the other hand, the wake structure behind the bubble for $\theta_C=135^o$ and $\theta_C=180^o$ (Fig. 6a,b) are very similar and thereby the drag.

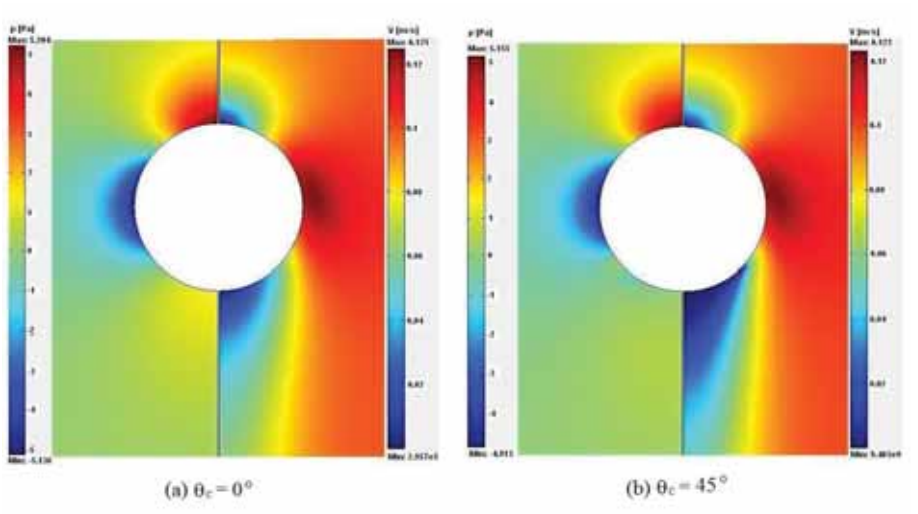

Fig. 5. Pressure and velocity field around the bubble for Re=100 and (a) θ_C=0º and (b) θ_C=45º

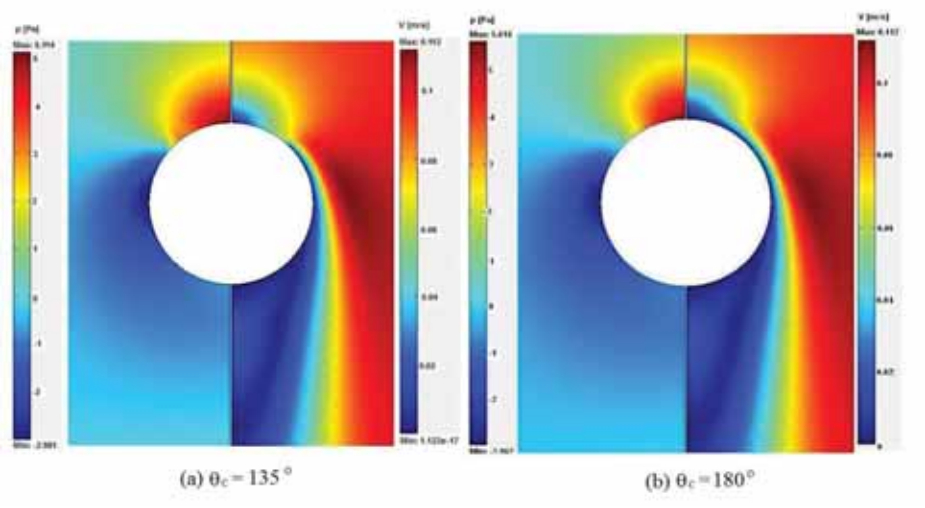

Fig. 6. Pressure and velocity field around the bubble for Re=100 and (a) θ_C=135º and (b) θ_C=180º

Figs. 7 and 8 shows the velocity and pressure magnitude values along the transversal direction to the undisturbed flow at outer up (Fig. 7a and 8a), up (Fig. 7b and 8b), down (Fig. 7c and 8c) and outer down (Fig. 7d and 8d) positions (see Fig 1), for the same Reynolds value than Figs. 5 and 6. As can be seen, the increase in the contamination angle from 0º to 45º and from 135º to 180º has no important effect in both the velocity and pressure, which is in contrast with the increasing from 0º to 90º. Because the integration of the fluid pressure and velocity distribution over the bubble surface gives the normal (form drag) and the tangential force (friction drag) over the bubble surface, both fluid-dynamics variable explains the cause why the drag is not increased in the same proportion as contamination angle increased. Thus, the approach and results presented in this work can be useful for an integral understanding of the effect of contamination grade on bubble´s drag.

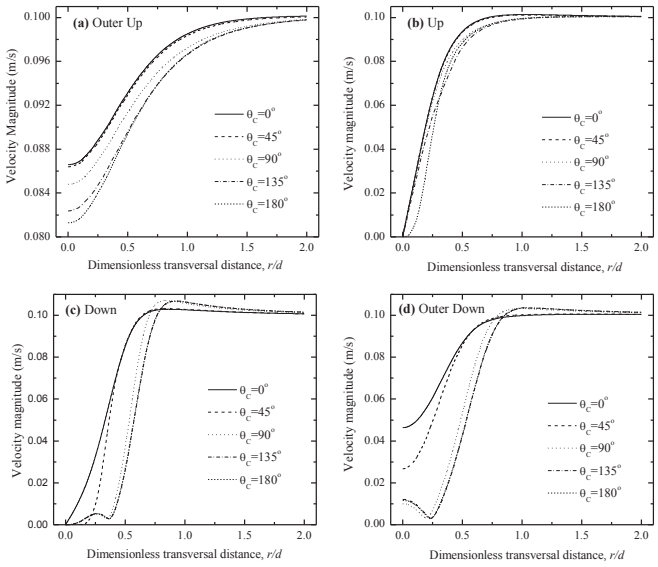

Fig. 7. Velocity magnitude along the transversal direction to the flow for (a) Outer Up, (b) Up, (c) Down and (d) Outer Down positions, for Re=100.

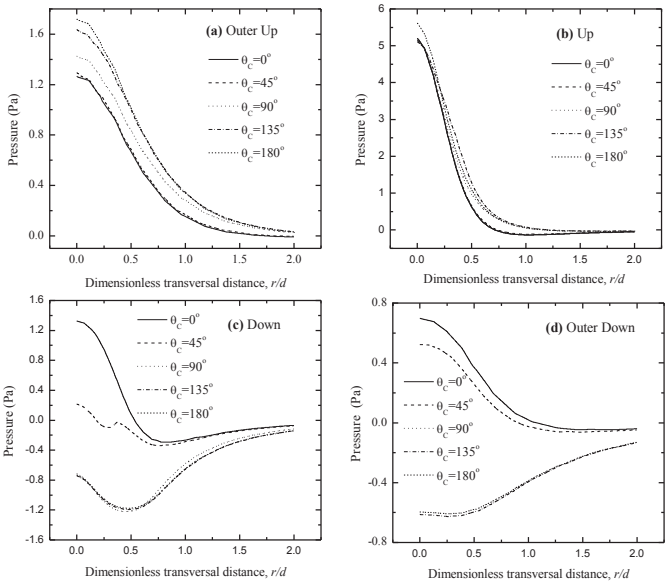

Fig. 8. Pressure field along the transversal direction to the flow for Outer Up (a), Up (b), Down (c) and Outer Down positions, for Re=100

4. Conclusions

The drag on a spherical bubble rising stationary in a liquid contaminated with surfactants and the wake structure behind the bubble were investigated in this work. The model solved in the present work considers the stagnant cap hypothesis, where is considered that surface diffusion of surfactants is extremely weak compared to advection and steady conditions are reached, i.e. the advective term vanishes. A simple explicit drag law for contaminated bubbles as function of the stagnant cap angle which is valid for $50 \leqslant Re \leqslant 200$ was obtained. Additionally, the flow regime (Re) under which a recirculation zone is formed behind a spherical bubble was numerically determined for each extent of the angle of contamination. Comparison of the model predictions with existing data were performed, showing very good agreement. The simulations have revealed several interesting features concerning the drag on the bubble and the structure of the flow around the bubble as function of the grade of contamination when steady conditions are reached. Among them, the following are pointed out: (1) the drag on the bubble is dependent of the stagnant-cap angle, but is independent of the Reynolds number, (2) for $\theta_C = 65^o$, the drag on a contaminated bubble is the 98.22% of the drag on a rigid sphere, (3) for $\theta_C > 143$ the drag on the bubble exhibit a slight dependence on the grade of contamination and is like to the drag on a clean bubble.

References

[1] Magnaudet J, Eames I. The motion of high-Reynolds-number bubbles in inhomogeneous flows. *Ann Rev Fluid Mech* 2000;**32**:659-708.

[2] Takagi S, Matsumoto Y. Surfactants effects on bubble motion and bubbly flows. Annu. Rev. *Fluid Mech* 2011;**43**:615-636.

[3] Duineveld PC. The rise velocity and shape of bubbles in pure water at high Reynolds number. *J Fluid Mech* 1995;**292**: 325–332.

[4] Clift R, Grace JR, Weber ME. Bubble, drops and particles. Academic Press, New York; 1987.

[5] Levich VG. Physicochemical hydrodynamics. Prentice-Hall, Englewood Cliffs, NJ; 1949.

[6] Cuenot B, Magnaudet J, Spennato B. The effects of slightly soluble surfactants on the flow around a spherical bubble. *J Fluid Mech* 1997;**339**:25-53.

[7] Alves SS, Orvalho SP, Vasconcelos JMT. Effect of bubble contamination on rise velocity and mass transfer. *Chem Eng Sci* 2005;**60**:1-9.

[8] Palaparthi R, Papageorgiou DT, Maldarelli C. Theory and experiments on the stagnant cap regime in the motion of spherical surfactant-laden bubbles. *J Fluid Mech* 2006;**559**:1–44.

[9] Frumkin A, Levich V. On surfactants an interfacial motion. *Zhur Fiz Khim* 1947;**21**:1183-1204.

[10] Bird RB, Stewart WE, Lightfoot EN. Transport Phenomena. Wiley, New York; 1960.

[11] Moore DW. The boundary layer on a spherical gas bubble. *J Fluid Mech* 1963;**16**:161-176.

[12] Sadhal S, Johnson R. Stokes flow past bubbles and drops partially coated with thin films. *J Fluid Mech* 1983;**126**:237-250.

[13] Fdhila RB, Duineveld PC. The effect of surfactant on the rise of a spherical bubble at high Reynolds and Peclet numbers. *Phys Fluids* 1996;**8**:310-321.

[14] Landau L, Lifshitz E. Fluid Mechanics (Course of Theoretical Physics). Vol. 6, second ed. Butterworth Heinemann, Oxford; 1987.

[15] Ramírez-Muñoz J, Soria A. An expression for the hydrodynamic force on a body interacting with the leading body wake. *Rev Mexicana Ingen Quim* 2007;**6**:101-109.